

1 Sustainability of the coastal zone of the Ganges-Brahmaputra-Meghna delta under climatic and
2 anthropogenic stresses

3

4

5 Md. Munsur Rahman¹

6 Anisul Haque¹

7 Robert J Nicholls²

8 Stephen E Darby³

9 Mahmida Tul Urmi¹

10 Md. Maruf Dustegir¹

11 Frances E. Dunn⁴

12 Anika Tahsin¹

13 Sadmina Razzaque¹

14 Kevin Horsburgh⁵

15 Md. Aminul Haque⁶

16

17 ¹ Institute of Water and flood Management (IWFm), Bangladesh University of Engineering &
18 Technology (BUET), Dhaka, Bangladesh.

19 ² Tyndall Centre for Climate Change Research, University of East Anglia, Norwich UK

20 ³ School of Geography and Environmental Science, University of Southampton, Highfield, Southampton

21 ⁴ Faculty of Geosciences, Utrecht University, The Netherlands

22 ⁵ Green Climate Fund, 175 Art center-daero, Yeonsu-gu, Incheon 22004. Republic of Korea

23 ⁶ Water Resources Planning Organization (WARPO), Dhaka, Bangladesh

24

25

26

Abstract

The Ganges-Brahmaputra-Meghna (GBM) delta is one of the world's largest deltas. It is currently experiencing high rates of relative sea-level rise of about 5 mm/year, reflecting anthropogenic climate change and land subsidence. This is expected to accelerate further through the 21st Century, so there are concerns that the GBM delta will be progressively submerged. In this context, a core question is: can sedimentation on the delta surface maintain its elevation relative to sea level? This research seeks to answer this question by applying a two-dimensional flow and morphological model which is capable of handling dynamic interactions between the river and floodplain systems and simulating floodplain sedimentation under different flow-sediment regimes and anthropogenic interventions. We find that across a range of flood frequencies and adaptation scenarios (including the natural polder-free state), the retained volume of sediment varies between 22% to 50% of the corresponding sediment input. This translates to average rates of sedimentation on the delta surface of 5.5 mm/yr to 7.5 mm/yr. Hence, under present conditions, sedimentation associated with quasi-natural conditions can exceed current rates of relative sea-level rise and potentially create new land mass. These findings highlight that encouraging quasi-natural conditions through the widespread application of active sediment management measures has the potential to promote more sustainable outcomes for the GBM delta. Practical measures to promote include tidal river management, and appropriate combinations of cross-dams, bandal-like structures, and dredging.

Keywords: Ganges-Brahmaputra-Meghna delta, anthropogenic climate change, relative sea-level rise, sedimentation, sustainability.

1. Introduction

Lying at the transition between fluvial and coastal environments, deltas are dynamic environments that are changing constantly due to both climatic and anthropogenic factors ([Ericson et al., 2006](#); [Tessler et. al.,](#)

2015; Santos and Dekker, 2020). With an abundant supply of nutrients associated with fine-grained sedimentation, deltas therefore often have highly productive soils for agriculture and fisheries, as well as ease of transport, so they have long been attractive places for human settlement, urban development, and intensive economic activity (Woodroffe et al., 2006; Syvitski et al., 2009; Edmonds et al., 2020). However, many deltas are now experiencing severe anthropogenic stress (Nicholls et al., 2020; Vasilopoulos et al., 2021) resulting from, for example, the construction of upstream dams, the development of dikes and embankments, water and mineral extraction, habitat destruction, and significant land-use change. These interventions frequently perturb natural water and sediment dynamics, which results in promotion of land subsidence, salinity intrusion, water quality deterioration, and the reduction of accretion processes (Day et al., 1997; Nicholls et al., 2018; Rahman et al., 2020). In addition, climate-driven sea-level rise (SLR) further compounds the multiple stresses that contemporary deltas are facing (de Souza, 2015; Brown et al., 2018).

The Ganges-Brahmaputra-Meghna (GBM) delta, located at the northern margin of the Bay of Bengal, is administered by both India and Bangladesh. It is characterized by many livelihood opportunities, as well as biophysical and socio-economic challenges which are increasing due to rising climate and anthropogenic stress (Rahman et al., 2020; Marcinko et al., 2021; Das et al., 2021). The large input of freshwater, sediments, and nutrients, combined with the high saline water input forced by tides, underpin diverse ecosystem resources (Miah, 2010; Nicholls et al., 2018). The people living in the coastal belt are highly dependent on traditional monsoon rice cultivation, as well as activities such as riverine and marine fishing and honey collection. The coastal population is also exposed to climate hazards such as fluvio-tidal floods, and tropical cyclones accompanied by storm surges, as well as riverbank erosion, salinity intrusion due to seasonal low flow levels in rivers, upstream water diversions and land use impacts (Dastagir, 2015; Akter et al., 2019). The mean tidal range in Bangladesh varies from 3-4 m and the tide propagates up to 100 km inland (Choudhury and Haque 1990; Haque and Nicholls, 2018; Bricheno et al., 2016), yet the delta's low-lying areas have an average elevation of just 1-2 m above mean sea level, creating a situation where large areas of land are exposed to natural inundation. In addition, large areas of the delta are subsiding at 2-3

77 mm/yr ([Brown and Nicholls, 2015](#); [Becker et al., 2020](#)), further contributing to the submergence of the low-
78 lying areas of the coastal zone.

79 Until the 1950s, the tidal floodplain in the GBM delta (in Bangladesh) was strongly connected to the
80 river system, so that it functioned as a natural sedimentation basin. Local communities managed the
81 floodplain through construction of temporary low height earthen embankments during the eight dry months
82 of the year ([Gain et al., 2017](#)) to protect crops against salinity intrusion. These temporary embankments
83 were submerged during the monsoon flooding, thus enabling quasi-natural inundation and sedimentation
84 processes on the tidal floodplains. Additionally, these quasi-natural processes allowed hydrological flows,
85 sediment dispersion and elevation gain as part of the delta building process. However, during the 1960s-
86 1990s, 139 polders (that include more than 6000 km of earthen embankments) were constructed to protect
87 the land from salinity and flooding as part of an attempt to increase agricultural productivity, and as a result
88 contemporary land use within the poldered areas has become increasingly dependent on dike protection.
89 Therefore, the sediment inputs and sediment dispersion processes on the delta floodplain are now
90 significantly changed. Importantly, in areas where natural sedimentation has been disrupted, the polders
91 lose elevation relative to sea level which increases the threats of waterlogging, saline groundwater intrusion
92 and catastrophic damage if the dikes are breached. The rate of accretion in what is today a highly modified
93 GBM delta depends on how much incoming fluvial and/or marine sediment flux is retained on the delta
94 surface. The physical sustainability of the delta depends on the future rate of fluvial sediment supply ([Darby](#)
95 [et al., 2018; 2020](#)) and its dispersion processes ([Wilson et al., 2017](#)) through the channel networks that
96 intersect the delta surface. Recently, [Dunn et al \(2019\)](#) showed that the supply of fluvial sediment to the
97 GBM delta is likely to decline significantly in the future due to anthropogenic changes in the upstream
98 catchment.

99 If fluvial sediment supply declines, vertical accretion and its capacity to counter subsidence and SLR
100 is also likely to decrease ([Rahman et al., 2018](#); [Dunn et al, 2018](#)), potentially causing large areas of the delta
101 to progressively lose elevation, which is especially problematic for low-lying areas. This poses a substantial
102 and increasing hazard to the large rural population and their livelihoods as the elevation of the delta surfaces

103 they inhabit approaches, or falls below, mean sea level. Therefore, it is fundamental to understand the
104 changing trends of relative sea-level rise ($RSLR = \text{local rate of SLR} + \text{land subsidence}$) and the rate of delta
105 plain sedimentation (Day et al., 2008). It is widely recognized (Nowreen et al., 2014) that the non-
106 functionality of canals within poldered areas restricts flow and sedimentation and is, therefore, responsible
107 for sedimentation of riverbeds in the region outside the polders. The gradual fall of elevations inside polders
108 due to the absence of sediment input has created uneven elevations inside and outside of the polders, which
109 promotes water-logging-related problems (Noor, 2018). If saline water enters poldered regions during
110 cyclones, salinisation can occur for a prolonged period. As such, there is growing interest in evaluating
111 potential remedial measures including: (i) the restoration of the tidal plain functioning, and (ii) promoting
112 sediment ingress and retention into polders to raise the low-lying land, consistent with nature-based
113 approaches.

114 Before adopting such options, it is fundamental to understand how anthropogenic factors are
115 changing and what impacts those factors will have on delta functions. There are few system-level analyses
116 that address these issues, such as Rogers and Overeem (2017) who undertook numerical simulations of the
117 GBM delta using AquaTellus. However, the detailed hydrodynamics of the processes involved are not well
118 represented. In particular, the AquaTellus model cannot resolve the impacts of polders on overbank
119 flooding and resultant sediment deposition. In another study, a process-based, two-dimensional numerical
120 model using the Delft3D modelling platform was applied to undertake a range of simulations designed to
121 elucidate the impact of environmental changes and anthropogenic interventions such as fluvial water
122 discharge, sediment discharge, relative sea level rise, construction of polder-dykes and cross-dams
123 (Angamuthu et al., 2018). One of the study objectives was to understand the dynamics of the delta
124 morphology over multi-decadal timescales. It was observed that when individual drivers of change act in
125 combination, delta building processes such as the distribution of sediment flux, aggradation, and
126 progradation are disrupted by the presence of isolated interventions that eventually lead to growing
127 dependence on flood defenses and increasing impacts if they fail. In this context, the aim of this paper is to
128 quantify the sedimentation across the surface of the Ganges-Brahmaputra-Meghna delta and assess its

129 potential to counter RSLR. To do this we employ a large-scale numerical model to investigate the potential
130 for sedimentation across the delta for plausible combined scenarios of flooding and human intervention on
131 the delta. In contrast to the prior studies, these new simulations provide a more robust and realistic
132 representation of the hydrodynamic processes in the presence of polders.

133

134 **2. Methodology**

135 **2.1 Study Area and Methodological Framework**

136 The GBM basins and delta, with flows of water and sediment coming from the basins and draining
137 through the estuarine networks in the coastal region, are shown in [Figure 1](#). Eastern, central, and western
138 region of the estuarine system (henceforth EES, CES, and WES, respectively) are recognized, connected
139 through several cross channels. In addition, the seasonal variations of freshwater flow cause local variations
140 in water and sediment flows that ultimately lead to spatial and temporal variations of sedimentation within
141 the estuarine system ([Haque et al., 2016](#); [Dasgupta et al., 2014](#)).

142



Figure 1: River basins of the Ganges-Brahmaputra-Meghna and the estuarine systems of coastal Bangladesh. The inset figure shows the entire basins of the three major rivers – the Ganges, Brahmaputra, and Meghna. The zoomed view, as marked in the inset, shows the part of the basins which are in Bangladesh and the three estuarine systems – Western Estuarine System (WES), Central Estuarine System (CES) and Eastern Estuarine System (EES). The important rivers (Ganges, Brahmaputra-Jamuna, Meghna, Gorai, Arial Khan, Mathabanga, Madhumati), estuaries (Lower Meghna system), and connecting channels (Beel Route, Spill Channel-1, Spill Channel-2, Spill Channel-3, Ghashiakhali) within these estuarine systems are also shown. Four locations where sedimentation thickness was measured by Rogers et al. (2013) in the Sundarban region are shown by square box symbol, where location-1 is in Bagerhat district, location-2 is in Pirojpur district, location-3 is in Khulna district, and location-4 is in Satkhira district.

We seek to clarify the formative processes of the GBM delta system via quantification of the key parameters including SLR, subsidence, total incoming sediment, and its retention on the delta surface. With respect to quantification of the retention of sediment on the delta surface, we evaluate sediment dispersion processes, including estimation of the portion of incoming sediment load contributing to delta building and maintenance, and tidal floodplain sedimentation, using empirical data complemented by numerical experiments. The overall analytical framework enables the determination of effective sea-level rise (ESLR) in terms of vertical change of delta surfaces compared to local relative sea-level rise (RSLR) as defined by Equation (1):

$$ESLR = RSLR - A \quad (1)$$

where A is the aggradation rate determined from the volume of sediment retained on the subaerial delta surface as new sedimentary layers (Syvitski et al., 2009) in mm/yr, and $RSLR = \Delta E + NS$, where ΔE is the eustatic SLR (mm/yr) as determined from changes to the volume of the global ocean over time, and net subsidence (NS) is defined as $NS = CN + CA \pm M$ (with CN = natural compaction, CA = accelerated compaction that reduces the volume of deltaic deposits, and M = vertical movement of the land surface as influenced by the redistribution of Earth's masses). Therefore, positive values of ESLR in Equation (1) indicate a tendency for land submergence whereas negative values indicate the potential for emergence of new land.

Although attempts have been made recently to estimate the above parameters for a comparative risk assessment across different deltas (Tessler et al., 2017), analysis of specific deltas remains problematic because of the need to consider the effects of local infrastructure, such as the polders in coastal Bangladesh. Information on SLR and subsidence is available from the literature, but quantification of the retained portion of incoming sediment flux and its distribution on the delta surface is still an issue that needs to be systematically resolved. We therefore applied the morphological model of the Delft3D modeling suite to compute coastal floodplain sedimentation under four hydrological and anthropogenic scenario combinations (Hibma et al. 2003; Haque et al., 2016; WARPO-BUET, 2019), with field observations of sedimentation (Rogers et al., 2013; Rogers and Overeem, 2017) used for model calibration and validation.

The delta-surface sedimentation for each of these scenarios is then calculated in conjunction with estimates of sea-level rise and subsidence to evaluate effective sea-level rise for each scenario.

2.2 Assessment of Sedimentation

To assess the aggradation rate (A in Equation (1)), the two-dimensional module of the Delft3D flow and morphology model is applied to estimate the retained volume of sediment and the area of the inundated subaerial delta surface. The Delft3D morphology model is dynamically coupled with the flow model, therefore any changes in the river and floodplain morphology that affect the flow field and *vice versa* are simulated. We have selected a two-dimensional model over one-dimensional (*which considers flow as unidimensional and does not consider momentum transfer between the river-floodplain systems*) and three-dimensional (*which is more relevant to resolve the local flow dynamics in detail*) to accommodate dynamic interaction between the river and floodplain systems, lateral dispersion and diffusion processes, and floodplain sedimentation. The two-dimensional module of Delft3D is widely used, with a long track record in different environments including oceans, coastal environments, estuarine and river systems all over the world (Thanh et al., 2019; Sandbach et al., 2018; Hu et al., 2018; Salehi, 2018; Li et al. 2018; Bennett et al., 2018) including many applications in Bangladesh (Haque, et al., 2016; WARPO and BUET, 2019; Akter et al., 2019; Al Azad et al., 2018; Haque et al., 2018).

2.2.1 Model Description

The model domain consists of the coastal region of Bangladesh that includes land, river, and sea area (Figure 2). The model is bounded in the north by the major rivers of the system (Ganges, Brahmaputra, and Meghna) and in the south by the Bay of Bengal (Figure 2). A variable mesh size is used with a coarser grid size (approximately $500\text{m} \times 600\text{m}$) in the sea area and finer grid size (approximately $200\text{m} \times 300\text{m}$) in the land area to capture the details of river, estuary, and land topography. All the rivers and estuaries within this region which have a width greater than or equal to 100m is included in the model domain. The coastal zone contains 139 polders, of which 103 are located within the study region based on the polder

map available from the National Water Resources Database (NWRD) of WARPO. The locations of
polders with actual and design dike heights are provided in the supplementary material (Figure S1).

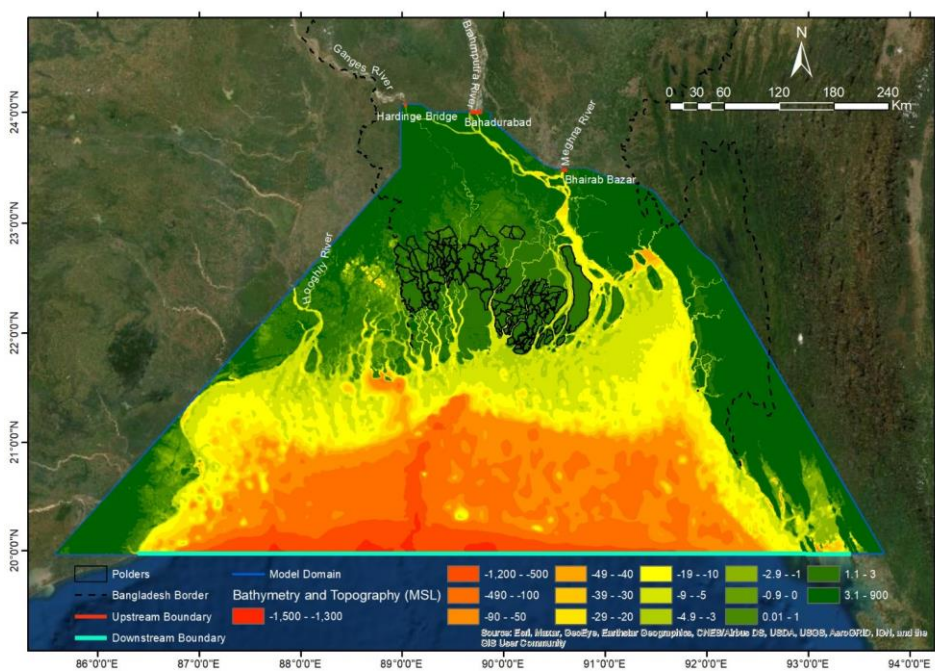


Figure 2: The model domain, including the major rivers, topography and bathymetry. The topography and bathymetry are measured in meters from Mean Sea Level (MSL). The model domain covers the coastal part of the Ganges-Brahmaputra-Meghna delta, and the Bangladesh territory is shown by black dotted lines. Locations of the three upstream river discharge boundaries and the downstream sea level boundaries are marked. The black firm lines represent the polders.

The model parameters which are used during model simulations are: (1) Manning’s resistance coefficient; (2) sediment density; (3) water density; (4) median sediment size; (5) hindered and non-hindered settling velocities; (6) vertical diffusion coefficient; (7) sediment concentration and concentration gradient in the bottom layer; (8) erosion parameter; and (9) critical shear stress for erosion and deposition.

220 During model simulations, the different size fractions of sediment, including mixtures of non-cohesive and
221 cohesive sediments, are considered. Based on [Rogers and Overeem \(2017\)](#), the distribution of cohesive and
222 non-cohesive sediments was selected as 70% cohesive and 30% non-cohesive for this study region. In all
223 the numerical experiments, two contrasting flooding conditions were used – an ‘average’ and an ‘extreme’
224 flood condition. For the average flood condition, measured data at the three upstream boundary locations
225 ([Figure 2](#)) were used for the year 2000 (January 1 to December 31). For the extreme flood condition,
226 measured data were used for the year 1998 (January 1 to December 31).

227 Details of the model is provided in the [supplementary material](#) as: model equations for the water and
228 sediment transport processes ([Section S.1](#)), model data sources ([Section S.2](#)), model boundary conditions
229 ([Section S.3](#)), model parameters ([Section S.4](#)), values of the calibration parameters ([Table S1](#)), and values
230 of the model parameters used in the numerical experiments ([Table S2](#)).

231

232 2.2.2 Model Calibration and Validation

233 The only sedimentation data available for model calibration is from [Rogers et al. \(2013\)](#) for the
234 Sundarbans. During model calibration, constant values were used for the following model parameters across
235 the entire model domain: (1) water and sediment properties; (2) settling velocity of cohesive sediment; (3)
236 maximum sediment concentration for hindered settling; (4) bottom layer thickness; (5) erosion parameter;
237 and (6) critical shear stress for erosion and deposition. However, these values may vary to an unknown
238 extent in the other regions of the coastal zone, so during calibration we applied uncertainty ranges to the
239 following spatially variable parameters: (1) space-varying resistance coefficients; (2) space varying
240 diffusion coefficients; (3) space varying sediment concentration; and (4) concentration gradients. These
241 parameters largely dictate the flooding and sedimentation processes across the study area. The resistance
242 co-efficient is the dominant model parameter determining the spatial variability of flow and sedimentation
243 processes. Manning’s co-efficient is used in the model as the resistance coefficient and is varied in this
244 study from a minimum of 0.00025 in the ocean to a maximum of 0.10 in the Sundarbans region (see the
245 [supplementary material, Table S1](#)). Ocean is a wide water body where bottom resistance has little influence

to flow and sedimentation processes (resistance co-efficient = 0.00025). Resistance slowly increases towards the estuary and rivers (varies from 0.015 to 0.025). Floodplain flow and sedimentation processes are largely influenced by the land-use types, which are represented by a variable resistance coefficient (0.025 close to estuary/river and increasing to 0.040 further inland). Depending on the forest cover, flow velocity decreases in the Sundarbans region. Denser forest cover is used near the coast (resistance coefficient = 0.1) to a lighter forest cover more inland (resistance coefficient = 0.08). The diffusion coefficient determines the turbulent transport of suspended sediment (Equation S1 in the supplementary material). Spatial distribution of suspended sediment concentration is not available in the study area. To take account of this uncertainty, we employed a spatially varying diffusion coefficient between 1-10 m²/s, which ensures the optimal calibration result (supplementary material, Table S1). Solution of the transport equation (Equation S1 in the supplementary material) with this diffusion coefficient gives space varying suspended sediment concentrations and concentration gradients for the entire study region. Values of all the model calibration parameters used here are summarized in the supplementary material (Table S1).

The model was calibrated using field data from March-October 2008 (Rogers et al., 2013), as shown in Figure 3. Two different methods were used to calculate sedimentation during this calibration period:

- (a) Method-1: Annual sedimentation based on the simulation from March-October (monsoon season), following Rogers et al. (2013).
- (b) Method-2: Annual sedimentation based on a simulation for the whole year (monsoon and dry seasons).

Except for location-4, Method-1 performs better than Method-2 (Figure 3), which means that the model performs better when the same time period is applied in the model to that which is used in the field (Rogers et al., 2013). Sedimentation is generally low in Method-2 (the 12-month simulation) compared to Method-1 (8 months of simulation from March to October i.e. during the monsoon) except for location-3. Method-2 includes the dry season period when erosion is dominant over sedimentation due to the low sediment inflow into the system and regular tidal flooding on the floodplain. Location-3 (located in Khulna district, see Figure 1) receives more sediment due to the clockwise residual circulation pattern in the Bay of Bengal

near the coast generated from the Coriolis force (Haque et al., 2016). Although Method-1 performs better in the context of model calibration, in this study we have used Method-2 to simulate annual sedimentation in the study region to also consider the effects of the dry season.

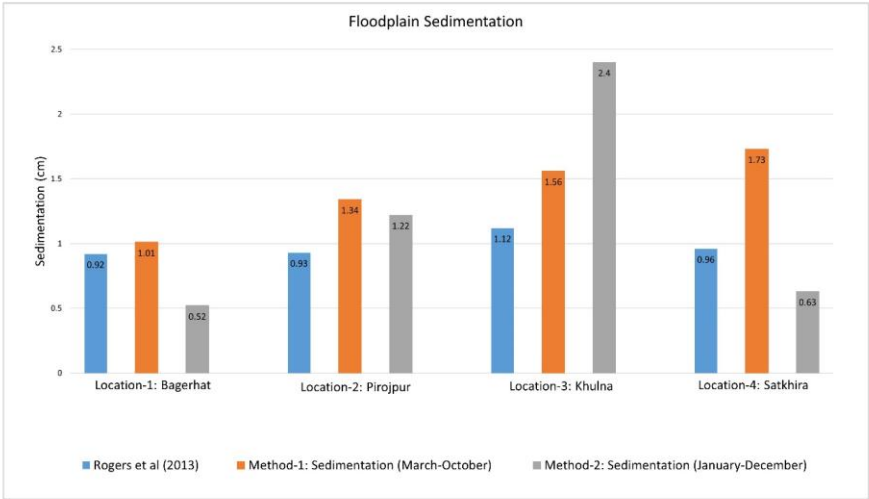


Figure 3: Comparison of floodplain sedimentation in the Sundarban region between modelled and measured data (Source of measured data: Rogers et al., 2013). All the measurement locations are in Sundarban region (see Figure 1). Location-1 is in Bagerhat district, location-2 is in Pirojpur district, location-3 is in Khulna district, and location-4 is in Satkhira district. Method-1 shows the sedimentation for 8 months model simulation (March-October) whereas, Method-2 shows the sedimentation for 12 months model simulation (January-December). Both the measurement and the model simulations are for the year 2008.

To validate the model, the simulated sediment load deposited on the floodplain was compared with estimated data (keeping all other data, parameters, and assumptions unchanged from the values used during the model calibration in Method-2). Goodbred and Kuehl (1998) and Allison (1998) estimate that 30-40%

288 of the total sediment entering the system is deposited over the floodplain. Although these two studies are
 289 not specific for any flood condition, for model validation we compared the model simulation for average
 290 flood conditions with their estimated value due to absence of any other data. Specifically, the percentage
 291 of sediment load deposited over the different floodplain systems (WES, CES and EES, see [Figure 1](#)) and
 292 the total sediment load computed for the entire study region is shown in [Table 1](#). Out of a total sediment
 293 load of 400 Million Tonnes entering the system during an average flood year, 90 Million Tonnes (~22%)
 294 are deposited on the floodplain of the study region according to the model. The WES is predicted to receive
 295 the greatest portion, followed by the CES and EES. The fact that the model predicts a higher retention
 296 potential for the CES over the EES is realistic due to the absence of polders in the central region, which
 297 allows greater sedimentation. The high retention for the WES reflects that sediment is readily trapped inside
 298 the high resistance Sundarbans Forest system where polders are completely absent.

303 [Table 1](#): Comparison of model-simulated retention of sediment on the delta plain and observations of
 304 [Goodbred and Kuehl \(1998\)](#) and [Allison \(1998\)](#) during an average flood year. The delta plain is divided
 305 into three estuarine systems – Western Estuarine System (WES), Central Estuarine System (CES), and
 306 Eastern Estuarine System (EES). All sediment loads are expressed in Million Tonnes (MT).

Total sediment input (MT)		400
Tidal floodplain region	Sediment load deposited (MT)	Approximate percentage of total load retained
WES	46	11%
CES	27	7%
EES	17	4%
Total (Model)	90	22%
Total (Goodbred and Kuehl, 1998 ; Allison, 1998)	124 to 165	30% - 40%

2.2.3 Outline of the Numerical Experiments

In this study, simulations using the Delft3D flow and morphological models were used to compute the impacts of polders on floodplain sedimentation in the study area. Four numerical experiments were conducted, categorized broadly as two states of the system: a ‘natural state’ and an ‘intervened state’ under two different flooding conditions – an ‘average flood’ with a return period of 2.33 years and an ‘extreme flood’, with a return period of 200 years. The ‘natural state’ represents the physical setting when there is no human intervention in the system. The ‘intervened state’ represents the physical system with the existing polder embankments constructed in the system. Further, the ‘average flood’ represents a flood condition when 20% to 22% of the total floodplain in the country is inundated, while the ‘extreme flood’ represents a flooding condition for which more than 60% of the total floodplain is inundated (BWDB, 2015).

2.3 Assessment of Sea-Level Rise and Subsidence

We compiled sea-level rise data for the Bay of Bengal region from global sources and used an estimate consistent with values used in Bangladesh national planning. Presently, climate-induced sea-level rise is ~ 3 mm/year and subsidence is ~ 2 mm/year, giving present RSLR as ~ 5 mm/year (Brown and Nicholls, 2015; Becker et al., 2020). This RSLR value is used as a reasonable estimate of the minimum future value in the GBM delta (BDP 2100, 2018; IPCC, 2019) and is compared with the sedimentation thickness obtained from the numerical experiments using Equation 1.

3 Results

3.1 Numerical Experiments-Group 1: Flooding and Sedimentation in an Intervened State

In the ‘intervened state’, we modelled two scenarios of inundation and corresponding sedimentation reflecting the average (Figure 4a and 4c) and extreme flood conditions (Figure 4b and 4d). Sedimentation occurs in those parts of the floodplain where sediment-laden flood water can enter. During a flood event, water can only enter a polder when the water depth outside the embankment exceeds the specified embankment height. Only a few of the polder embankments in the north of the region are overtopped during

the average and extreme flood conditions (Figures 4a and 4b). Indeed, no polders at all are overtopped in the central region (part of CES) or in the Sundarbans (part of WES). In the CES region during average flood conditions, inundation and sedimentation are confined within the low elevation area (Figures 4a and 4c). In the same region, both inundation and sedimentation extend to a larger area during the extreme condition (Figures 4b and 4d). In the Sundarbans region, inundation and sedimentation during extreme flood condition (Figures 4b and 4d) is substantially higher than during the average flood condition (Figures 4a and 4c).

In general, the numerical experiments for this ‘intervened’ condition highlight the effectiveness of polder embankments in preventing inundation in the region for a wide range of flood conditions. Hence, sedimentation only occurs in the unprotected regions outside the polder embankments and, to a limited extent, in the region where floodwater overtops the embankments. An important observation is that during the extreme flood condition the sedimentation is much higher when compared to the average flood condition (Figures 4c and 4d). The resulting volume of sediment retained on the delta surface during an ‘extreme’ flood is also higher (~ 500 MT, which is approximately 42% of the incoming sediment during an extreme flood) compared to the ‘average’ flood condition (~ 90 MT, which is approximately 22% of the incoming sediment during average flood). One of the important hydraulic reasons for such enhanced sedimentation in the extreme flood condition within the coastal zone of Bangladesh is that the sediment transport capacity does not increase proportionately with the increase of water discharge and sediment flow because of the extensive flat land elevations and associated low longitudinal slope. This creates a sediment surplus in excess of transport capacity and therefore, more sediment is likely to be deposited (Haque et al., 2016) with the increase of flow-sediment in the GBM system. However, as the return period for the extreme flood event is large (200 years), it is unlikely that very large magnitude floods contribute significantly to delta building processes in the longer term.

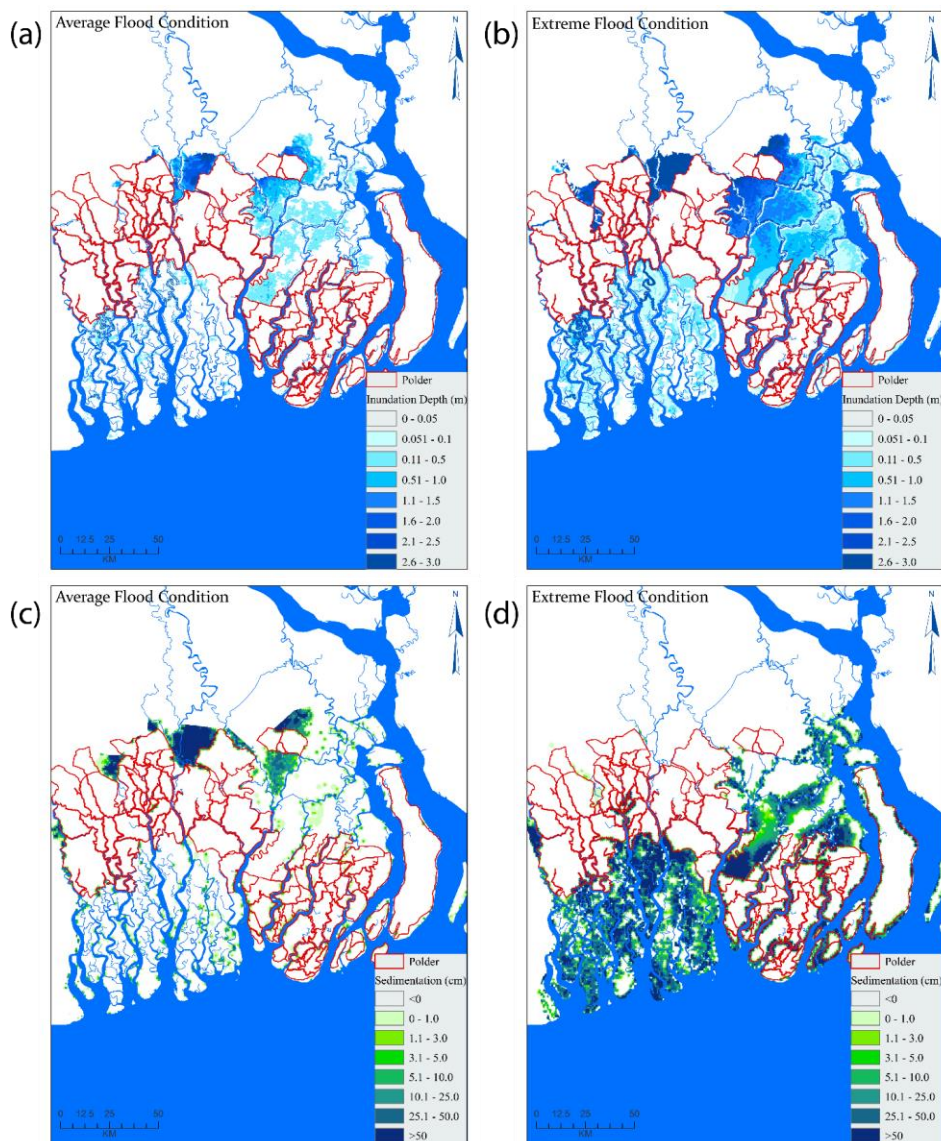


Figure 4: Maximum inundation (4a and 4b) and annual sedimentation (4c and 4d) in the intervened delta state during average flood and extreme flood conditions, respectively. The red lines show the polder embankments. Only part of the unprotected land is inundated during average flood condition (4a). The

extent and severity of inundation increases with the intensity of flooding (4b). Sedimentation occurs in the areas which are flooded (4c and 4d). Following the inundation patterns, sedimentation only occurs on part of the inundated land (4c) and increases with the depth and area of inundation (4d).

3.2 Numerical Experiments-Group 2: Flooding and Sedimentation in a Natural State

The numerical experiments represent a pre-disturbance delta, before polders were constructed in the region (pre-1960 condition). All the major, intermediate, and minor rivers and their interconnections are represented as in the present-day condition. This allows fluvial, fluvio-tidal, and tidal flooding in the floodplain of the system to be represented in a hypothetical natural state under present-day conditions. The hydrodynamics and sedimentation in the system are governed by the exchange of flow between the floodplain and riverine/estuarine systems. As expected, the simulations for the natural state show inundation across a wider area for both flood conditions. As sedimentation occurs in the inundated regions, a wider area experiences sediment deposition in the natural state as compared to the intervened state (see Figures 4 and 5). In the numerical experiment for the average flood condition, areas in the natural state are flooded and sedimented (Figures 5a and 5c) which were protected in the intervened state (Figures 4a and 4c). The extreme flood condition shows how effective the polder embankments are in protecting the region against inundation. Without polder embankments, the entire region is inundated during the extreme flood condition (Figure 5b), with a much wider area experiencing sedimentation (Figure 5d). The maximum zone of sedimentation is again found to be in the Sundarbans and its northern area (Figure 5d). The area north of the Sundarbans is well known as a water-logged area due to polder embankments which restrict sedimentation on the floodplain inside the protected region (WARPO and BUET, 2019). This group of numerical experiments show that without these polder embankments, sedimentation would otherwise occur in what is today a sediment-starved floodplain.

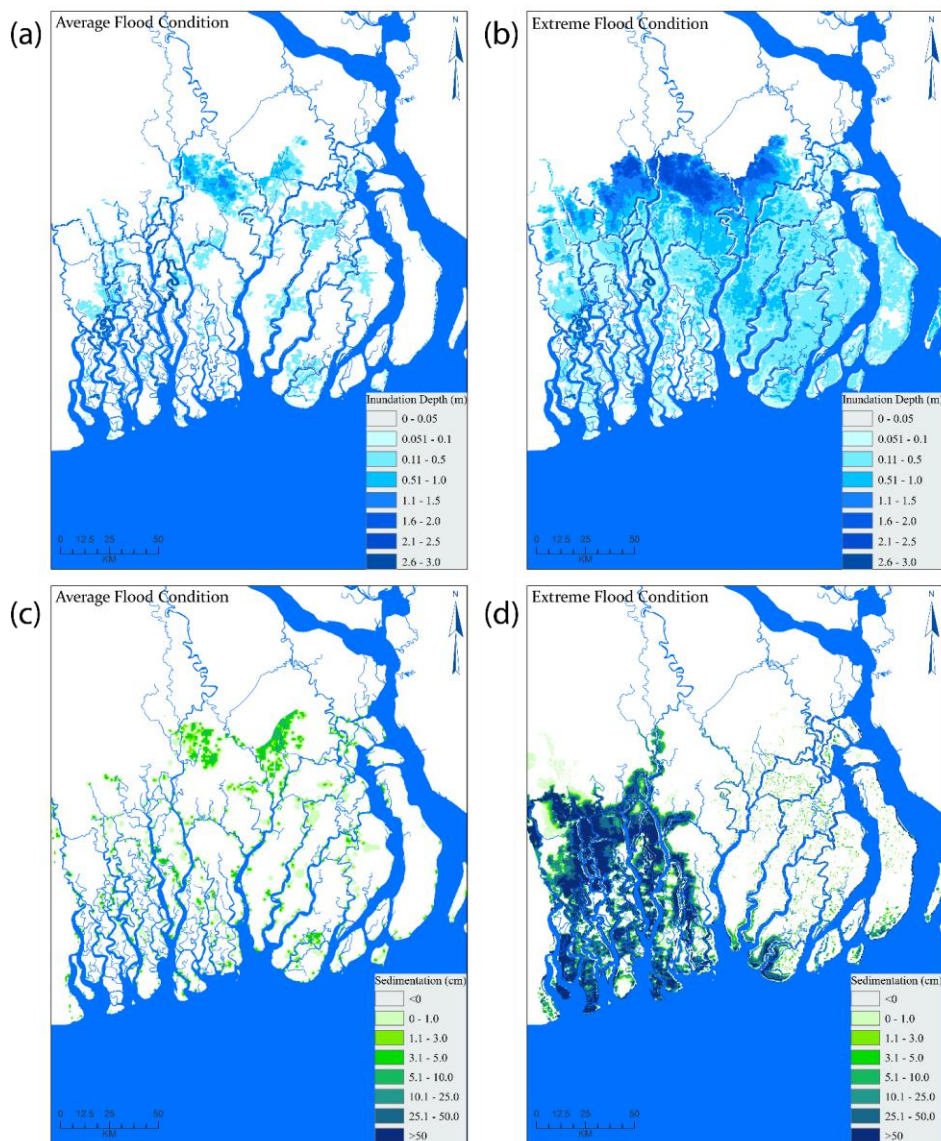


Figure 5: Maximum inundation (5a and 5b) and annual sedimentation (5c and 5d) in the natural delta state for average flood and extreme flood conditions. The inundation of the delta in the natural state depends entirely on the flooding condition, existing river and canal bathymetry, and land topography: less

391 *inundation during an average flood condition (5a) as compared to an extreme flood condition (5b). For*
392 *average flood conditions, sedimentation occurs in the delta region where inundation depth is relatively*
393 *high (5c). For extreme flood conditions, higher flow resistance in the Sundarban region increases*
394 *sedimentation (5d).*

395

396 **3.3 Characteristics of Sedimentation on the Delta Surface based on the Numerical Experiments**

397 Basic characteristics of sedimentation on the delta surface are quantified based on two groups of
398 numerical experiments described in [Section 3.1](#) and [3.2](#). Ranges of yearly average values for different flood
399 conditions and for different physical settings of the delta, as characterized by the following parameters, are
400 computed to describe the characteristics of sedimentation in the delta - total sediment input, sedimented
401 area, sediment retained on the floodplains, and sedimentation thickness ([Table 2](#)). The lower value of the
402 range for all the parameters in [Table 2](#) represents the average flood condition, while the upper value
403 represents the extreme flood condition. The range of values also represent different physical settings of the
404 delta (intervened or natural). It is expected that during any flood event and for varying sediment
405 management scenarios in the delta, the values of the parameters will vary in the ranges defined in [Table 2](#).
406 For example, during any flood event, total sediment input in the system varies between 400 MT to 1200
407 MT depending on the frequency of the flood event ([Table 2](#)). Due to this flood event and sediment inflow
408 to the system, total sediment volume deposited in the floodplain varies between 90 MT to 600 MT, which
409 is 22% to 50% of the total incoming sediment volume.

410 The maximum fraction (30 MT to 340 MT, which is 8% to 28% of the inflow sediment volume) of
411 the sediment is deposited on the CES where there are no polders even during the intervened state of the
412 delta. The next highest area of sedimentation is the WES (45 MT to 260 MT, which is 11% to 21% of the
413 inflow sediment volume) which is dominated by the Sundarbans. Although sediment input is almost similar
414 for the WES and CES, unlike the CES, the WES is a heavily intervened system (except the Sundarbans
415 region) causing uneven distribution of sediments inside and outside the polders. As mentioned in [section](#)
416 [3.2](#), this causes waterlogging in most parts of the WES. Among the three systems, the area of minimum

417 sedimentation is the EES (17 MT to 25 MT, which is 2% to 4% of the inflow sediment volume). The EES
418 and CES are dominated by the freshwater systems of the Lower Meghna while the WES is dominated by
419 the saline water estuarine systems (Figure 1). Sources of sediments in the WES are therefore different from
420 the CES and EES. The WES receives marine sediments which re-enter into the system through oceanic
421 circulation (Haque et al., 2016), while the CES and EES receive riverine sediments from the Lower Meghna
422 system (Figure 1). These aspects determine the non-uniform spatial variation of sediment distribution in
423 the delta, resulting in variations of sedimentation thickness on the delta surface (5.5 mm to 7.5 mm) that
424 depend on the flood condition and physical setting of the delta.

425 The physical setting of the delta (intervened or natural) also dictates the sediment retained on the
426 delta surface, which varies from 23 MT to 107 MT (6% to 9% of the corresponding sediment inflows)
427 spreading over a sedimentation area that varies from 1922 km² to 3720 km² (30% to 31% of the
428 corresponding intervened state) depending on the flood condition. As mentioned before, all the high-end
429 values in the parameter ranges of Table 2 represent the extreme flood condition. It is unlikely that such a
430 low probability extreme event (with 200 years return period) would be considered in any sediment
431 management plan because the severity of the flood would be unacceptable to society. However, as these
432 high-end values are also associated with the natural state of the delta, the physical state of the delta plays
433 an important role in determining the most appropriate sediment management plan. It is important to note
434 that in the natural state of the delta a greater amount of sediment is retained within the extended area, which
435 is essential to ensure delta building processes in a uniform way.

436
437
438
439
440
441
442

Table 2: Ranges of total sediment input, sedimentation area, retained sediment and sedimentation thickness on the inundated delta surface based on the numerical experiments. The entire coast is divided into three estuarine systems – Western Estuarine System (WES), Central Estuarine System (CES), and Eastern Estuarine System (EES). Sediment input and sediment retained on the floodplains are expressed as annual average values in Million Tonnes (MT).

Annual Average Values		Entire Coast	WES	CES	EES
Total sediment input (MT)		400 to 1200			
Sediment retained on the floodplains (MT)		90 to 600	45 to 260	30 to 340	17 to 25
Percentage of total sediment input retained		22% to 50%	11% to 21%	8% to 28%	2% to 4%
Average sedimentation thickness (mm)		5.5 to 7.5			
Change from intervened to natural state	Increase of retained sediment (MT)	23 to 107 (6% to 9% increase)			
	Increase of sedimentation area (km ²)	1922 km ² to 3720 km ² (30% to 31% increase)			

4. Discussion

4.1 Impacts of Polders on Coastal Flooding and Sedimentation

Our numerical experiments demonstrate that sedimentation thickness on the delta surface depends on the inflow sediment volume, and the retained sediment fraction on the floodplains. Within the same physical settings, the incoming flow and sediment flux during extreme floods is much higher than the flow and sediment flux during the average flood. During both the average and extreme flood conditions in the intervened state, the numerical experiments successfully simulate the prototype observations as sedimentation is mainly confined to the unprotected areas outside the polders. This results in an uneven

land building process, which is one of the main reasons for waterlogging inside the polders. However, the observed phenomenon did not happen overnight as the poldered embankments were implemented gradually over a period of three decades. The timing of the water-logged area has been compared with the corresponding poldered area in recent research (Noor, 2018). The study revealed that around 30% of the study area was poldered by the 1970s, increasing gradually to around 60% by the 1990s. Meanwhile, the water-logged area increased from 2% to 5% during the period mentioned above. Since then, the water-logged area increased to around 35% by the year 2016. In addition to the impacts of polders as mentioned above, one of the reasons for the sharp increase of water-logged area within a comparatively short time is inappropriate design and/or poor maintenance of the drainage facilities inside polders.

In contrast, in the natural state, the same volume of floodwater and sediments that enter the region are dispersed over a larger area with more uniform sedimentation. These findings highlight the potential benefits of restoration of quasi-natural conditions to develop sustainable sediment management in the coastal systems of the GBM delta (Wilson et al., 2017; WARPO and BUET, 2020; WARPO and BUET, 2021), especially in the WES (Table 2) which currently has a high density of poldered embankments and suffers waterlogging driven by uneven sedimentation.

4.2 Potential for Enhancing Sediment Retention on Delta Surface

The natural delta state retains sediment on the delta surface in relatively uniform fashion. Depending on the flood condition and intervened state of the delta, the percentage of retained sediments varies from 22% to 50%, with a sedimentation thickness of 5.5 mm/yr to 7.5 mm/yr (Table 2). Therefore, for any flood condition and for any physical state of the delta, the model-simulated sedimentation thickness exceeds the synthesized value of RSLR in this study (5 mm/yr) and the average sediment supply is sufficient to maintain the relative elevation. However, if the sediment supply increases, sedimentation rates would have the potential to further exceed RSLR and create new elevated areas in the delta.

However, to materialize the inherent opportunities (such as land reclamation) and counter different challenges (such as siltation in navigational routes, and salinity-flooding-water logging in cultivable lands),

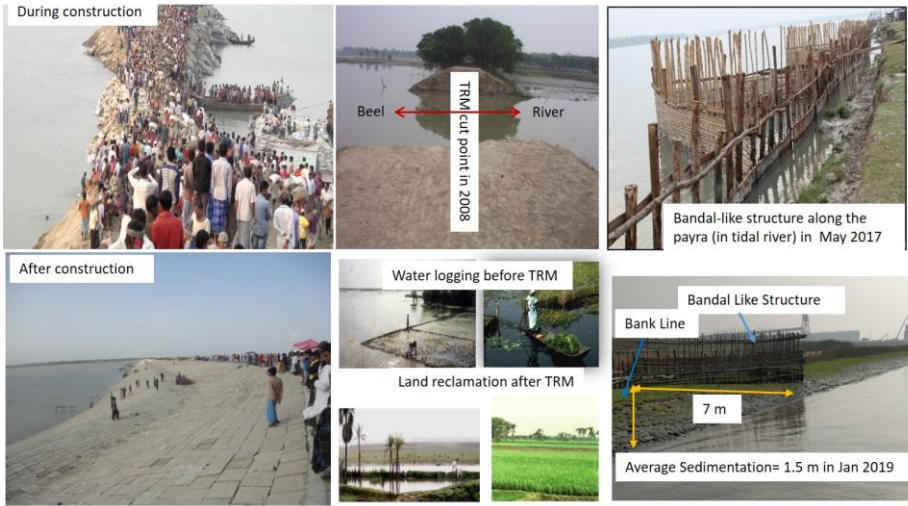
485 various interventions are being practiced in the coastal zone that can generate unwanted consequences even
486 while fulfilling the specific objectives. Broadly, the practiced methods can be divided into two categories:
487 (i) management to accelerate siltation and (ii) management to promote de-siltation. In the first category,
488 cross-dams and tidal river management (TRM) are usually implemented for land reclamation and to elevate
489 land, while in the second category dredging often complements the use of bandal-like structures that are
490 adopted for the maintenance of navigational channels and landing ports. However, the history, working
491 principles and functionalities for each of the methods are different and these techniques are typically applied
492 in isolation to achieve the goals of the specific projects. Some examples of cross-dams, TRM and bandal-
493 like structures are shown in Figure 6 and discussed briefly below:

494 **Cross-dams** are closure structures employed to increase the residence time of marine sediment to
495 enhance sedimentation and are often used for land reclamation between the mainland and islands ([World](#)
496 [Bank, 2012](#); [Paul and Rashid, 2017](#)). Several implementations of such structures have been undertaken by
497 the BWDB ([personal communication](#)) and have achieved successful land reclamation. Examples include
498 the Noakhali Cross-dam 1 in 1957, the Noakhali Cross-dam 2 in 1964, followed by the Muhuri closure dam
499 in 1985, that together have created more than 1000 km² of land. Following the success of these projects, a
500 further 19 cross-dam priority sites have been identified by BWDB with the objective of accelerating the
501 natural processes of land accretion. For example, 4 km² of new land has been reclaimed by the construction
502 of Char Montaz-Char Khalifa (known as Bestin Closure) in 2009-2010, while the Char Islam-Char Montaz
503 cross-dam was constructed in 2014-2015 and reclaimed 2 km² land. More recently, in 2015, a cross-dam
504 was constructed at the estuary of Sandwip Channel over Little Feni river and 3 km² of land has been created
505 downstream. However, these advantages are accompanied by inherent drawbacks, such as high instability
506 and potential for continuous change and variability that creates new challenges elsewhere under the altered
507 flow-sediment regime; this affects the existing hydrological conditions and need to be addressed carefully
508 in such as dynamic system ([World Bank, 2012](#); [WARPO and BUET, 2020](#)). While cross-dams cause local
509 sedimentation, it is important to note that at the delta-scale there is no net gain in land accretion – rather
510 cross-dams redistribute sedimentation at the delta scale ([Angamuthu et al., 2018](#)).

To assess the potential impact of several cross-dams proposed by BWDB, a recent study ([WARPO and BUET, 2021](#)) examined the system impacts of these cross-dams by applying process-based numerical model in GBM delta. The study found that these cross-dams, if implemented simultaneously in isolation with other sediment management practices (for example TRM or dredging), changes the tidal hydrodynamics of the GBM systems which may result a long term morphodynamic impact. As most of these cross-dams are planned within the zone of turbidity maximum (EES region), trapped sediments due to these cross-dams cause less sediments to be supplied in the western estuary systems (WES region) and lead to riverbed erosion in this region. At the same time, the increased sedimentation in the cross-dam locations decreases the channel conveyance and cause additional flooding in the regions impacted by cross-dams. The study also found that due to additional retained sediment by these cross-dams, the resulting sedimentation thickness in south-central region (CES) is reduced. The impact of this decreased sedimentation thickness plays a significant role on delta sustainability when compared in [Table 2](#). As we mentioned before, cross-dam and similar sediment management practices although can fulfill the local objectives but may prove to produce unwanted impacts in other regions of the delta.

As discussed earlier with reference to the previous studies, and as further confirmed in the numerical experiments undertaken here, the poldered embankments have de-coupled the floodplains from the peripheral rivers, preventing sediment flow into the poldered areas and ultimately creating elevation differences between the inside and outside of polders; such elevation differences driving waterlogging inside polders.

Tidal River Management (TRM) has been practiced since the 1990s to get relief from such waterlogging. TRM involves the periodic cutting and closing of polder embankments at strategic locations to increase the residence time of the sediment rich tidal flow volume and hence accelerate land accretion (or reclamation) inside low lying poldered areas (locally known as *beels*). TRM also acts to naturally dredge the river which is connected to the TRM system (river-polder-connecting channel-*beel*). However, to solve the problem in a sustainable way in the long-run, such operations are to be shifted dynamically in different low-lying areas which needs prior socio-technical analysis ([Rocky et al., 2020](#)).



(a) Musapur Cross-dam 2015 (BWDB) (b) TRM operation in beel Khuksia during 2006-2011 (CEGIS) (c) Land reclamation using bandal-like structures in Payra river (Kibriya, 2020)

538

539 **Figure 6:** Field examples of cross-dam (left), TRM (middle) and bandal-like structures (right) as practiced
540 in Bangladesh's coastal zone. Cross-dams are a labor-intensive construction as it needs to utilize the
541 specific tidal phase to construct the main barrier (left-top photo) and later transforms into a permanent
542 structure (left-bottom photo). For TRM, the man-made canal connects the river with the beel (middle-top
543 photo). Due to TRM operation, the natural dredging of the river solves the waterlogging problem (middle-
544 mid photo) and at the same time, fills the beel with sediments causing building of new land (middle-bottom
545 photo). Bandal-like structures are made with eco-friendly soft materials (right-top photo) to stabilize the
546 riverbank with reclaimed land and increase the conveyance capacity of the river (right-bottom photo).

547

548 **Bandal-like Structures** are indigenous nature-based solution that are primarily utilized for de-
549 siltation along navigational channels, through redistributing the flow-sediment regime to create a sediment
550 deficit zone (within the navigational channels) and a sediment surplus zone (along the bankside). To utilize
551 the power of the flow-sediment regime in bi-directional tidal environments, the shape of the structure is

typically modified from a single to double limb (Rahman et al., 2020; Kibriya, 2020) with appropriate opening and inclination that can be utilized for the maintenance of navigational channels and bank stabilization, simultaneously.

River dredging is widely used in Bangladesh for the maintenance of navigational depths in rivers and ports, reduce inundation, and has recently been applied to solve waterlogging problems within polders. However, the impact of dredging is very temporary (WARPO and BUET, 2020). And being costly, the sustainability of dredging is questionable when a long-term morphological time scale is considered. As the riverine and estuarine systems of the delta are interconnected, it is not unlikely that dredging in a specific river/estuary has the potential to change the flow-sediment equilibrium of the system and may change zones of sedimentation on the delta surface, as observed in the numerical experiments undertaken here.

From the above examples, both cross-dams and TRM are implemented to accelerate sedimentation, bandal-like structures are employed to accelerate both siltation and de-siltation, and dredging is employed to increase navigational depth, reduce inundation, and solve waterlogging problem. Such ad-hoc measures that are geared primarily towards solving local problems may contribute to further uneven distribution of delta development processes (Wilson and Goodbred, 2015) and may cause long-term morphodynamic change in the delta (WARPO and BUET, 2021). Moreover, it is not possible to return back to the delta's natural state because the infrastructures are now an essential component to the local people in protecting their land from flooding and salinity intrusion (Rahman et al., 2021). The technical insights of the locally adaptive indigenous methods have already been clarified through a number of research projects (Hussain et al., 2018; Adnan et al., 2020; Rahman et al., 2004; Zhang et al., 2010; Kibriya, 2020) and some of the above methods (Figure 6) have been tested for sediment management purposes in the south-west region of Bangladesh in isolation and have shown mixed experiences of failures/successes with emerging socio-technical challenges (Hussain et al., 2018; Adnan et al., 2020). For any specific sediment management practice or combination of different practices, local impacts often extend outside the domains under investigation and the entire system needs to be considered in an integrated way using a single modelling

577 framework with continuous feedback of data (Bangladesh Delta Model, [WARPO and BUET, 2020](#);
578 [WARPO and BUET, 2021](#)) to enable understanding of the system response to the implemented options.

579

580 **4.3 Potential to Increase Basin Scale Incoming Sediment Flux**

581 It has been shown that sediment input to the GBM system is still sufficient to counterbalance the
582 present rate of RSLR and more, hence there is currently potential for the development of additional land
583 mass in the delta system. However, the observed and expected decline of total incoming sediment load
584 ([Rahman et al, 2018](#); [Duun et al, 2018](#); [Dunn et al., 2019](#)), as well as the acceleration of climate-induced
585 sea-level rise ([IPCC, 2021](#)), reduce the future potential to counterbalance land submergence in the coastal
586 region of Bangladesh. Moreover, for the strongest mitigation scenario in AR6 the median climate-induced
587 sea-level rise is about 50 cm over the remaining 80 years of this century, that is about 6 mm/yr and RSLR
588 in Bangladesh might increase to 8 mm/yr. Maintaining elevation will therefore require a lot more sediment.
589 Comparatively, based on long term data measured by BWDB, the estimated recent sediment load is found
590 to have been lowered by almost 50% below the average value usually expected in Bangladesh (1 billion
591 tonnes) and is further decreasing at a rate of 10 MT/year ([Rahman et al., 2018](#)). However, considering a
592 range of scenarios of climate change (that are typically likely to produce more sediment load) and
593 anthropogenic interventions (which are likely to intercept more sediment thus produce less sediment load),
594 future sediment fluxes are projected to decrease at a slower rate of around 5 MT/year ([Dunn et al., 2018](#)).
595 Therefore, it can be assumed that the sediment supply in the GBM system is likely to decline and the
596 potential for offsetting RSLR will also decline over time. Moreover, with a reduced sediment supply to the
597 system, the rivers and coasts will likely experience new challenges related to fresh land loss.

598 Furthermore, it has long been observed that a large number of basin-scale water diversion structures
599 have already been implemented to meet the needs for socio-economic development in each of the countries
600 sharing the rivers within the GBM systems ([Grumbine and Pandit, 2013](#); [Dunn et al, 2018](#)). The primary
601 objective of such water diversion structures is to withdraw water from the main flow and divert it to water
602 deficit regions, but a side-effect of these structures is that they intercept incoming sediment flows ([Foufoula,](#)

2013). The conventional head control structures for water and sediment flows over the diversion structures can be revised through introducing nature-friendly technology, for example Piano Key Weirs (PKW) over which sediments can be lifted by turbulence to reduce sediment interception (Machiels et al., 2010; Abhash and Pandey, 2021). Likewise, more innovative basic research is required to adopt appropriate head control elements over the existing and upcoming water control infrastructure. The recently developed system level modelling framework, the Bangladesh Delta Model (BDM), which integrates the entire processes of ocean, coast, Sundarbans, polders, canal network, estuaries, inland rivers of different scales, embankments, wetlands, beels and haors of the Bangladesh delta can be an important vehicle to test potential sediment management options (WARPO and BUET, 2020; WARPO and BUET, 2021) and has further potential to be integrated with existing hydrological models, such as BDWRM (Salehin et al., 2011) that use gridded rainfall data in GBM basins. BDWRM is a hydrological model, but it has the potential to incorporate the sediment flow over prescribed head control structures. The recent understanding of the common threats and possible solutions could facilitate the engagement of policymakers to create opportunities for co-learning to resolve the problems of the shared GBM delta in Bangladesh and India through joint research (Das et al., 2021; Rahman et al, 2020).

4.4 Wider Implications to the Coastal Zone of the GBM Delta

The coastal zone of the GBM delta is one of six hotspots subject to several hazards including unwanted sedimentation and erosion (BDP 2100, 2018). Many infrastructural projects are planned to be implemented across the course of this century, including ports, economic zones, power plants, and tourist spots, and as part of national development and adaptation against climate change (MoEF, 2009; NAPA 2009) new landmass is a pre-requisite for these developments. The results of this present study indicate that incoming sedimentation thicknesses do have potential to maintain the delta elevation above the RSLR, albeit with varying potential in each of the regions. To maximize the sustainable use of these natural resources, identification of different development project sites should consider the trade-off between the natural potential of sedimentation and the development need of the country. The sediment quality is another

629 issue to consider, for example (the western system) (the Sundarbans) receives marine sediment which re-
630 enters into the system from upstream rivers by traveling through the saline sea, so these sediments are
631 predominantly saline. On the other hand, the central and eastern systems receive freshwater riverine
632 sediments from the Lower Meghna systems. As a result, the ecosystem productivity, livelihood adaptations,
633 and development opportunities in the western system are different from the central and eastern systems.

634 However, most of the development projects in the delta do not take into account this vital
635 information and therefore the knowledge generated in the present research will add value to the Bangladesh
636 Delta Plan 2100 for the effective implementation of future projects. A national strategy for sediment
637 management needs to be introduced in the BDP 2100 based on the latest research on the GBM delta,
638 including lessons learned from other deltas such as the Mekong Delta in Vietnam (Dunn and Minderhoud,
639 2022). In addition, uncertainties of the future projections of SLR, precise estimates of spatially distributed
640 subsidence, and consideration of the entire GBM in a seamless modeling framework are to be explored in
641 upcoming research.

642

643

644 5. Conclusions

645 The question of whether sedimentation on the surface of the GBM delta in Bangladesh can maintain
646 its elevation relative to sea level is answered quantitatively in this paper using a calibrated and validated
647 two-dimensional numerical model, developed using the Delft3D modelling platform. Large scale numerical
648 experiments are performed by using average and extreme flood conditions combined with the natural and
649 the existing intervened states of the delta. The main conclusions are:

- 650 • In the intervened state, sedimentation only occurs in the unprotected regions (outside the polders),
651 while in the natural state the floodwater and sediments are dispersed and re-distributed over a larger
652 area (~ 30% larger) resulting in relatively more uniform sedimentation.
- 653 • The total annual volume of retained sediment on the delta surface varies between 22% and 50% of
654 the incoming sediment input between the intervened and natural states and average to extreme flood

Commented [DF(1)]: What does this mean?

conditions. As a result, average sedimentation on the delta surface exceeds the present value of RSLR (~5 mm/year) in all cases. Sedimentation is lower and shows more variability across the delta in the intervened state.

- Sedimentation can be enhanced by promoting a quasi-natural state. This can be achieved by controlled management of the flow-sediment regime using measures such as tidal river management (TRM), cross-dams, dredging, and bandal-like structures. This would capture more sediment and establish more uniform distribution of sedimentation inside and outside of the polders. Implementing such measures through monitoring the responses, preferably, using a system level model developed, has the potential to promote sediment management in the GBM delta and hence its physical sustainability in the long time.

The methodology developed in this study can be replicated in other similar deltas to analyze the physical sustainability of these vulnerable environments under variable sediment and flood regimes.

Acknowledgements

Collecting the bathymetry data was supported by the ‘ESPA Deltas ([NE/J002755/1](#))’ project supported by the ESPA programme, funded by the Department for International Development (DfID), the Economic and Social Research Council (ESRC) and the Natural Environment Research Council (NERC), UK, and the National Water Resources Database hosted at Water Resources Planning Organization (WARPO), Ministry of Water Resources (MoWR), Government of the People’s Republic of Bangladesh (GoB). The model development was supported by the DECCMA Project ([Grant No. IDRC 107642](#)), part of the Collaborative Adaptation Research Initiative in Africa and Asia (CARIAS), with financial support from the UK Government’s DfID and the International Development Research Centre (IDRC), Canada, the [WARPO Projects](#), ‘Research on the Morphological processes under Climate Changes, Sea Level Rise and Anthropogenic Intervention in the coastal zone’ and ‘Research on Sediment Distribution and Management in South-West Region of Bangladesh’ funded from MoWR, GoB and the ACCORD project ([NE/R000123/1](#)) funded by the UK NERC (through National Oceanographic Center, NOC).

References

- Abhash, A., Pandey, K.K. 2021. Experimental and Numerical Study of Discharge Capacity and Sediment Profile Upstream of Piano Key Weirs with Different Plan Geometries. *Water Resour Manage* 35, 1529–1546, <https://doi.org/10.1007/s11269-021-02800-y>
- Adnan MSG, Talchabhadel R, Nakagawa H, Hall JW. 2020. The potential of Tidal River Management for flood alleviation in South Western Bangladesh. *Sci Total Environ*. 2020 Aug 20;731:138747. doi: 10.1016/j.scitotenv.2020.138747. Epub 2020 May 6. PMID: 32438086.
- Akter, R.; Asik, T.Z.; Sakib, M.; Akter, M.; Sakib, M.N.; Al Azad, A.S.M.A.; Maruf, M.; Haque, A.; Rahman, M.M. 2019. The Dominant Climate Change Event for Salinity Intrusion in the GBM Delta. *Climate* 7, 69. <https://doi.org/10.3390/cli7050069>
- Al Azad, A.S.M.A., Mita, K.S., Zaman, M.W., Akter, M., Asik, T.Z., Haque, A., Hussain, M.A., Rahman, M.M., 2018. Impact of tidal phase on inundation and thrust force due to storm surge, *Journal of Marine Science and Engineering*, 2018, 6, 110; doi:10.3390/jmse6040110.
- Allison, M. A., 1998. Historical changes in the Ganges-Brahmaputra Delta front. *Journal of Coastal Research* 14 (4): 1269–1275.
- Angamuthu, B., Darby, S.E. and Nicholls, R.J., 2018. Impacts of natural and human drivers on the multi-decadal morphological evolution of tidally-influenced deltas. *Proceedings of the Royal Society A*, 474 (2219), 1-26. (doi:10.1098/rspa.2018.0396).
- BDP 2100, 2018. Baseline Studies on Water Resources Management. General Economic Division. Government of the People's Republic of Bangladesh
- Becker et al., 2020. Water level changes, subsidence, and sea level rise in the Ganges–Brahmaputra–Meghna delta, 117 (4) 1867-1876; first published January 6, 2020; <https://doi.org/10.1073/pnas.1912921117>.
- Becker, R.H. and Sultan, M., 2009. Land subsidence in the Nile Delta: inferences from radar interferometry. *The Holocene*, 19(6), pp.949-954.

706 Bennett, V. C., Mulligan, R. P., & Hapke, C. J., 2018. A numerical model investigation of the impacts of
 707 Hurricane Sandy on water level variability in Great South Bay, New York. *Continental Shelf Research*,
 708 161, 1-11.

709 Bimal Kanti Paul and Harun Rashid (2017), Coastal Landform Changes: Coastal Erosion, Land Accretion
 710 and Subsidence, Climatic Hazards in Coastal Bangladesh, Butterworth-Heinemann, Pages 121-152, ISBN
 711 9780128052761, <https://doi.org/10.1016/B978-0-12-805276-1.00004-1>.

712 Biswas, H., S.K. Mukhopadhyay, S. Sen, T.K. Jana. 2007. Spatial and temporal patterns of methane
 713 dynamics in the tropical mangrove dominated estuary, NE coast of Bay of Bengal, India, *Journal of Marine*
 714 *Systems* 68 (2007) 55–64.

715 Bricheno, L.M., Wolf, J. and Islam, S., 2016. Tidal intrusion within a mega delta: An unstructured grid
 716 modelling approach. *Estuarine, Coastal and Shelf Science*, 182, pp.12-26.
 717 <https://doi.org/10.1016/j.ecss.2016.09.014>

718 Brown S., Nicholls R.J, Lázár A., Sugata H., Appeaning Addo K., Hornby D.D., Hill C., Haque A., Caesar
 719 J. and Tompkins E., 2018. What are the implications of sea-level rise for a 1.5°C, 2°C and 3°C rise in global
 720 mean temperatures in vulnerable deltas? *Regional Environmental Change* 18(6), 1829-1842.

721 Brown, S. and Nicholls, R.J., 2015. Subsidence and human influences in mega deltas: the case of the
 722 Ganges–Brahmaputra–Meghna. *Science of the Total Environment*, 527, pp.362-374.

723 BWDB. 2015. *Annual flood report 2015*. Dhaka: Bangladesh Water Development Board (BWDB).
 724 <http://www.fwc.gov.bd/index.php/reports/annual-floodreports>. Accessed 9 May 2016.

725 BWDB. 2019. *Annual flood report 2019*. Dhaka: Bangladesh Water Development Board (BWDB).
 726 <http://www.fwc.gov.bd/images/annual19.pdf>. Accessed 7 June 2021.

727 Cazenave, A. and Nerem, R.S., 2004. Present-day sea level change: Observations and causes. *Reviews of*
 728 *Geophysics*, 42(3).

729 CCC, 2016. Assessment of Sea Level Rise on Bangladesh Coast through Trend Analysis. Climate Change
 730 Cell (CCC), Department of Environment, Ministry of Environment and Forests, Dhaka, Bangladesh.

731 Choudhury, J.U., and A. Haque. 1990. Permissible water withdrawal based upon prediction of salt-water
 732 intrusion in the Meghna delta. *The hydrological basis for water resources management proceedings of the*
 733 *Beijing symposium*. Publication no. 197. Wallingford: International Association of Hydrological Sciences
 734 (IAHS).

735 Darby S.E., Appeaning Addo K., Hazra S., Rahman M.M., Nicholls R.J., 2020. Fluvial Sediment Supply
 736 and Relative Sea-Level Rise. In: Nicholls R., Adger W., Hutton C., Hanson S. (eds) *Deltas in the*
 737 *Anthropocene*. Palgrave Macmillan, Cham. https://doi.org/10.1007/978-3-030-23517-8_5

738 Darby S.E., Nicholls R.J., Rahman M.M., Brown S., Karim R., 2018. A Sustainable Future Supply of
 739 Fluvial Sediment for the Ganges-Brahmaputra Delta. In: Nicholls R., Hutton C., Adger W., Hanson S.,
 740 Rahman M., Salehin M. (eds) *Ecosystem Services for Well-Being in Deltas*. Palgrave Macmillan, Cham.
 741 https://doi.org/10.1007/978-3-319-71093-8_15

742 Das, Shouvik, Hazra, Sugata, Haque, Anisul, Rahman, Munsur, Nicholls, Robert J., Ghosh, Amit, Ghosh,
 743 Tuhin, Salehin, Mashfiqu and Safra De Campos, Ricardo. 2021. Social vulnerability to environmental
 744 hazards in the Ganges-Brahmaputra-Meghna delta, India and Bangladesh. *International Journal of Disaster*
 745 *Risk Reduction*, 53. ISSN 2212-4209, DOI: 10.1016/j.ijdr.2020.101983

746 Dasgupta, S., Huq, M., Khan, Z.H., Ahmed, M.M.Z., Mukherjee, N., Khan, M.F. and Pandey, K., 2014.
 747 Cyclones in a changing climate: the case of Bangladesh. *Climate and Development*, 6(2), pp.96-110.

748 Dastagir, M. R. 2015. Modeling recent climate change induced extreme events in Bangladesh: A review.
 749 *Weather and Climate Extremes*, 7, 49–60. <https://doi.org/10.1016/j.wace.2014.10.003>.

750 Day Jr, J.W., Martin, J.F., Cardoch, L. and Templet, P.H., 1997. System functioning as a basis for
 751 sustainable management of deltaic ecosystems. *Coastal Management*, 25(2), pp.115-153.

752 Day, J.W., Christian, R.R., Boesch, D.M., Yáñez-Arancibia, A., Morris, J., Twilley, R.R., Naylor, L. and
 753 Schaffner, L., 2008. Consequences of climate change on the ecogeomorphology of coastal wetlands.
 754 *Estuaries and Coasts*, 31(3), pp.477-491.

755 Douglas A. Edmonds, Rebecca L. Caldwell, Eduardo S. Brondizio, Sacha M. O. Siani, 2020. Coastal
 756 flooding will disproportionately impact people on river deltas, NATURE COMMUNICATIONS,
 757 <https://doi.org/10.1038/s41467-020-18531-4>

758 Dunn, F.E. and Minderhoud, P. S. J., 2022. Sedimentation strategies provide effective but limited mitigation
 759 of relative sea-level rise in the Mekong delta, COMMUNICATIONS EARTH & ENVIRONMENT,
 760 <https://doi.org/10.1038/s43247-021-00331-3>

761 Dunn, F.E., Darby, S.E., Nicholls, R.J., Cohen, S., Zarfl, C. and Fekete, B.M., 2019. Projections of
 762 declining fluvial sediment delivery to major deltas worldwide in response to climate change and
 763 anthropogenic stress. *Environmental Research Letters*, 14(8), p.084034. (doi:10.1088/1748-9326/ab304e).

764 Dunn, F.E., Nicholls, R.J., Darby, S.E., Cohen, S., Zarfl, C. and Fekete, B.M., 2018. Projections of
 765 historical and 21st century fluvial sediment delivery to the Ganges-Brahmaputra-Meghna, Mahanadi, and
 766 Volta deltas. *Science of the total environment*, 642, pp.105-116. (doi:10.1016/j.scitotenv.2018.06.006).

767 Erban, L.E., Gorelick, S.M. and Zebker, H.A., 2014. Groundwater extraction, land subsidence, and sea-
 768 level rise in the Mekong Delta, Vietnam. *Environmental Research Letters*, 9(8), p.084010.

769 Ericson, J.P., Vörösmarty, C.J., Dingman, S.L., Ward, L.G. and Meybeck, M., 2006. Effective sea-level
 770 rise and deltas: causes of change and human dimension implications. *Global and Planetary Change*, 50(1),
 771 pp.63-82.

772 Foufoula-Georgiou, E. et al. (34 co-authors). 2013. A vision for a coordinated international effort on delta
 773 sustainability. In: Deltas: Landforms, Ecosystems and Human Activities. Proceedings of HP1, IAHS-
 774 IAPSO-IASPEI Assembly, Gothenburg, Sweden, (IAHS Publ. 358, 2013).

775 G. Vasilopoulos, Q.L. Quan, D.R. Parsons, S.E. Darby, V.P.D. Tri, N.N. Hung, I.D. Haigh, H.E. Voepel,
 776 A.P. Nicholas and R. Aalto. 2021. Establishing sustainable sediment budgets is critical for climate-resilient
 777 mega-deltas, Environ. Res. Lett. in press <https://doi.org/10.1088/1748-9326/ac06fc>

778 Gain, A. K., Benson, D., Rahman, R., Datta, D. K., & Rouillard, J. J. 2017. Tidal river management in the
 779 south west Ganges-Brahmaputra delta in Bangladesh: Moving towards a transdisciplinary approach?
 780 Environmental Science and Policy, 75, 111–120. <https://doi.org/10.1016/j.envsci.2017.05.020>

781 Goodbred, S.L. and Kuehl, S.A., 1998. Floodplain processes in the Bengal Basin and the storage of Ganges–
 782 Brahmaputra river sediment: an accretion study using ¹³⁷ Cs and ²¹⁰ Pb geochronology. *Sedimentary*
 783 *Geology*, 121(3), pp.239-258.

784 Goswami, D.C., 1985. Brahmaputra River, Assam, India: Physiography, basin denudation, and channel
 785 aggradation. *Water Resources Research*, 21(7), pp.959-978.

786 Gregory, J.M., Church, J.A., Boer, G.J., Dixon, K.W., Flato, G.M., Jackett, D.R., Lowe, J.A., O'farrell,
 787 S.P., Roeckner, E., Russell, G.L. and Stouffer, R.J., 2001. Comparison of results from several AOGCMs
 788 for global and regional sea-level change 1900–2100. *Climate Dynamics*, 18(3), pp.225-240.

789 Grumbine, R. E. and Pandit, M. K., 2013. Threats from India's Himalaya Dams, VOL 339 SCIENCE
 790 (www.sciencemag.org), pp 36-37.

791 Han, W., Meehl, G.A., Rajagopalan, B., Fasullo, J.T., Hu, A., Lin, J., Large, W.G., Wang, J.W., Quan,
 792 X.W., Trenary, L.L. and Wallcraft, A., 2010. Patterns of Indian Ocean sea-level change in a warming
 793 climate. *Nature Geoscience*, 3(8), p.546.

794 Haque, A. and Nicholls, R.J., 2018. Floods and the Ganges-Brahmaputra-Meghna Delta. In: Nicholls R.,
 795 Hutton C., Adger W., Hanson S., Rahman M., Salehin M. (eds) *Ecosystem Services for Well-Being in*
 796 *Deltas*. Palgrave Macmillan, Cham

797 Haque, A., Sumaiya and Rahman, M., 2016. Flow distribution and sediment transport mechanism in the
 798 estuarine systems of Ganges-Brahmaputra-Meghna delta. *International Journal of Environmental Science*
 799 *and Development*, 7(1), p.22.

800 Hibma, A., De Vriend, H.J. and Stive, M.J.F., 2003. Numerical modelling of shoal pattern formation in
 801 well-mixed elongated estuaries. *Estuarine, Coastal and Shelf Science*, 57(5-6), pp.981-991.

802 Higgins, S., Overeem, I., Tanaka, A. and Syvitski, J.P., 2013. Land subsidence at aquaculture facilities in
 803 the Yellow River delta, China. *Geophysical Research Letters*, 40(15), pp.3898-3902.
 804 <http://doi.org/10.1098/rspa.2018.0396>

805 Hu, K., Chen, Q., Wang, H., Hartig, E. K., and Orton, P. M., 2018. Numerical modeling of salt marsh
 806 morphological change induced by Hurricane Sandy. *Coastal Engineering*, 132, 63-81.

807 Hussain, M.A., Hossain, M.A. and Haque, A., 2012. Hydro-meteorological Impact on Residual Currents
 808 and Salinity Distribution at the Meghna Estuary of Bangladesh. In *Coastal Environments: Focus on Asian*
 809 *Regions* (pp. 88-105). Springer, Dordrecht.

810 Hussain, N., Islam, Md. H., & Firdaus, F., 2018. Impact of Tidal River Management (TRM) for Water
 811 Logging: A Geospatial Case Study on Coastal Zone of Bangladesh. *Journal of Geoscience and Environment*
 812 *Protection*, 6, 122-132. <https://doi.org/10.4236/gep.2018.612009>

813 IPCC, 2019. Summary for Policymakers. In: IPCC Special Report on the Ocean and Cryosphere in a
 814 Changing Climate [H.- O. Pörtner, D.C. Roberts, V. Masson-Delmotte, P. Zhai, M. Tignor, E. Poloczanska,
 815 K. Mintenbeck, M. Nicolai, A. Okem, J. Petzold, B. Rama, N. Weyer (eds.)].

816 IPCC, 2021. Summary for Policymakers. In: *Climate Change 2021: The Physical Science Basis.*
 817 Contribution of Working Group I to the Sixth Assessment Report of the Intergovernmental Panel on
 818 Climate Change [Masson-Delmotte, V., P. Zhai, A. Pirani, S. L. Connors, C. Péan, S. Berger, N. Caud, Y.
 819 Chen, L. Goldfarb, M. I. Gomis, M. Huang, K. Leitzell, E. Lonnoy, J.B.R. Matthews, T. K. Maycock, T.
 820 Waterfield, O. Yelekçi, R. Yu and B. Zhou (eds.)]. Cambridge University Press. In Press.

821 Islam, M.R., Begum, S.F., Yamaguchi, Y., Ogawa, K., 1999. The Ganges and Brahmaputra rivers in
 822 Bangladesh: basin denudation and sedimentation. *Hydrol. Process.* 13: 2907–2923.
 823 [https://doi.org/10.1002/\(SICI\)1099-1085\(19991215\)13:17b2907::AIDHYP906N3.0.CO;2-E](https://doi.org/10.1002/(SICI)1099-1085(19991215)13:17b2907::AIDHYP906N3.0.CO;2-E).

824 IWM, 2009. Use Existing Data on Available Digital Elevation Models to Prepare Useable Tsunami and
 825 Storm Surge Inundation Risk Maps for the Entire Coastal Region, Volume-II: DEM, Landuse and Geo-
 826 morphology Maps. Institute of Water Modelling & Bangladesh Institute of Social Research, April 2009.

827 Jelgersma, S., 1996. Land subsidence in coastal lowlands. *Sea-Level Rise and Coastal Subsidence*,
 828 Springer Professional, pp.47-62, [https://www.springerprofessional.de/en/land-subsidence-in-coastal-](https://www.springerprofessional.de/en/land-subsidence-in-coastal-lowlands/13434762)
 829 [lowlands/13434762](https://www.springerprofessional.de/en/land-subsidence-in-coastal-lowlands/13434762)

830 Kay, R., 1993. Deltas of the world. ISBN 10: 0872629627 ISBN 13: 9780872629622 ASCE.

831 [Kibriya, N.A. 2020](#). Performance Evaluation of Bandal-Like Structures for Tidal River Flow and Sediment
832 Management, unpublished Msc thesis, Intitute of Water and Flood Management, Bangladesh University of
833 Engineering and Technology, Bangladesh.

834 [Kulp, S.A. and Strauss, B.H., 2019](#). New elevation data triple estimates of global vulnerability to sea-level
835 rise and coastal flooding. *Nature communications*, 10(1), pp.1-12.

836 [Laz, O.U. 2012](#). Morphological assessment of a selected reach of Jamuna river by using Delft3d model,
837 M.Sc Thesis, Department of Water Resources Engineering, Bangladesh University of Engineering and
838 Technology (BUET), Dhaka, Bangladesh, December, 2012.

839 [Li, X., Plater, A., & Leonardi, N., 2018](#). Modelling the transport and export of sediments in macrotidal
840 estuaries with eroding salt marsh. *Estuaries and coasts*, 41(6), 1551-1564.

841 [Machiels O., Erpicum S., Dewals B. J., Archambeau P. and Pirotton M. 2010](#). Piano Key Weirs: the
842 experimental study of an efficient solution for rehabilitation, Flood Recovery, Innovation and Response II,
843 WIT Transactions on Ecology and the Environment, Vol 133, doi:10.2495/FRIAR100091

844 [Matsumoto, K., Takanezawa, T., Ooe, M. 2000](#). Ocean tide models developed by assimilating
845 TOPEX/POSEIDON altimeter data into hydrodynamical model: A global model and a regional model
846 around Japan. *J. Oceanogr.*2000, 56, 567–581.

847 [Miah, G., Bari, N. and Rahman, A., 2010](#). Resource degradation and livelihood in the coastal region of
848 Bangladesh. *Frontiers of Earth Science in China*, 4(4), pp.427-437.

849 [Milliman J.D., Broadus J.M. and Gable F. 1989](#). Environmental and economic implications of rising sea
850 level and subsiding deltas: the Nile and Bengal examples, *Ambio*, 18 (1989), pp. 340-345

851 [Minderhoud, P.S.J., Erkens, G., Pham, V.H., Bui, V.T., Erban, L., Kooi, H. and Stouthamer, E., 2017](#).
852 Impacts of 25 years of groundwater extraction on subsidence in the Mekong delta, Vietnam. *Environmental*
853 *research letters*, 12(6), p.064006.

854 [MoEF, 2009](#). Bangladesh Climate Change Strategy and Action Plan 2009, Ministry of Environment and
855 Forest, Government of the People’s Republic of Bangladesh.

856 NAPA, 2009. National Adaptation Programme of Action, Ministry of Environment and Forest,
 857 Government of the People's Republic of Bangladesh

858 Nicholls, R.J., Adger, W.N., Hutton, C.W., and Hanson, S.E., 2020. Delta Challenges and Trade-Offs from
 859 the Holocene to the Anthropocene, R. J. Nicholls et al. (eds.), *Deltas in the Anthropocene*,
 860 https://doi.org/10.1007/978-3-030-23517-8_1

861 Nicholls, R.J., Hutton, C.W., Adger, W.N., Hanson, S.E., Rahman, M.M. and Salehin, M., 2018. Integrative
 862 Analysis for the Ganges-Brahmaputra-Meghna Delta, Bangladesh. In *Ecosystem Services for Well-Being*
 863 *in Deltas* (pp. 71-90). Palgrave Macmillan, Cham.

864 Noor, S., 2018. Investigation on polderization induced water logging and feasible adaptation measures in
 865 Dumuria upazila under Khulna district. Unpublished M.Sc Thesis. Bangladesh University of Engineering
 866 and Technology, <http://lib.buet.ac.bd:8080/xmlui/handle/123456789/5143>

867 Nowreen, S., Jalal M. R. and Khan M. S. A, 2014. Historical analysis of rationalizing South West coastal
 868 polders of Bangladesh, Water Policy 16 (2014) 264–279. doi: 10.2166/wp.2013.172

869 Pethick, J. and Orford J. D., 2013. Rapid rise in effective sea-level in southwest Bangladesh: Its causes and
 870 contemporary rates, Global and Planetary Change, Volume 111, 237-245,
 871 <https://doi.org/10.1016/j.gloplacha.2013.09.019>

872 Rahman et al., 2020. Performance Evaluation of Bandal-like Structures for Sediment Management in
 873 Braided Jamuna River, Proceedings of the 22nd IAHR-APD Congress 2020, Sapporo, Japan, [https://iahr-](https://iahr-apd2020.eng.hokudai.ac.jp/htdocs/static/mirror/proceedings/pdf/1-1-7.pdf)
 874 [apd2020.eng.hokudai.ac.jp/htdocs/static/mirror/proceedings/pdf/1-1-7.pdf](https://iahr-apd2020.eng.hokudai.ac.jp/htdocs/static/mirror/proceedings/pdf/1-1-7.pdf)

875 Rahman M.M. et al., 2020. Ganges-Brahmaputra-Meghna Delta, Bangladesh and India: A Transnational
 876 Mega-Delta. In: Nicholls R., Adger W., Hutton C., Hanson S. (eds) *Deltas in the Anthropocene*. Palgrave
 877 Macmillan, Cham. https://doi.org/10.1007/978-3-030-23517-8_2

878 Rahman, M. A., Dawes, L., Donehue, P. and Rahman, M. R., 2021. Cross-temporal analysis of disaster
 879 vulnerability of the southwest coastal communities in Bangladesh, Regional Environmental Change (2021),
 880 <https://doi.org/10.1007/s10113-021-01797-9>

881 Rahman, M. M., Nakagawa, H., Khaleduzzaman, A. T. M., Ishigaki, T., & Muto, Y., 2004. On the
 882 formation of stable river course. *Annals of Disas. Prev. Res. Inst., Kyoto Univ., No. 47 B*

883 Rahman, M., Dustegir, M., Karim, R., Haque, A., Nicholls, R.J., Darby, S.E., Nakagawa, H., Hossain, M.,
 884 Dunn, F.E. and Akter, M., 2018. Recent sediment flux to the Ganges-Brahmaputra-Meghna delta
 885 system. *Science of the total environment*, 643, pp.1054-1064.

886 Rahmstorf, S., 2007. A Semi-Empirical Approach to Projecting Future Sea-Level Rise. *Science* 315, 368–
 887 370. doi:10.1126/science.1135456

888 Richardson, J. F., and Zaki, W. N., 1954. Sedimentation and fluidisation: Part 1. *Trans. Inst. Chem. Eng.*,
 889 32, 35–53.

890 Rijn, L. C. van, 1993. Principles of Sediment Transport in Rivers, Estuaries and Coastal Seas. Aqua
 891 Publications, The Netherlands.

892 Rocky, T., Nakagawa, H. and Kawaike, K., 2020. Selection of Appropriate Shifting of Tidal River
 893 Management, A. Haque, A. I. A. Chowdhury (eds.), Water, Flood Management and Water Security Under
 894 a Changing Climate, Springer Nature Switzerland AG 2020, [https://doi.org/10.1007/978-3-030-47786-](https://doi.org/10.1007/978-3-030-47786-8_20)
 895 [8_20](https://doi.org/10.1007/978-3-030-47786-8_20)

896 Rogers, K. and Overeem, I., 2017. Doomed to drown? sediment dynamics in the human-controlled
 897 floodplains of the active Bengal Delta. *Elementa Science of the Anthropocene*, 5(65).

898 Rogers, K.G., Goodbred Jr, S.L. and Mondal, D.R., 2013. Monsoon sedimentation on the ‘abandoned’ tide-
 899 influenced Ganges–Brahmaputra delta plain. *Estuarine, Coastal and Shelf Science*, 131, pp.297-309.

900 Salehi, M., 2018. Storm surge and wave impact of low-probability hurricanes on the lower delaware bay—
 901 Calibration and application. *Journal of Marine Science and Engineering*, 6(2), 54.

902 Salehin Mashfiqus, Jahir Uddin Chowdhury and A.K.M. Saiful Islam, 2011. Basin wide and Regional Grid-
 903 Based Hydrologic Models for Ganges, Brahmaputra and Meghna River Systems, BUET and WARPO,
 904 Technical Report 02, R01/ 2011, February 2011.

905 Sandbach, S. D., Nicholas, A. P., Ashworth, P. J., Best, J. L., Keevil, C. E., Parsons, D. R., & Simpson, C.
 906 J., 2018. Hydrodynamic modelling of tidal-fluvial flows in a large river estuary. *Estuarine, Coastal and*
 907 *Shelf Science*, 212, 176-188.

908 Santos, M.J. and Dekker, S.C., 2020. Locked-in and living delta pathways in the Anthropocene. *Sci Rep*
 909 10, 19598 (2020). <https://doi.org/10.1038/s41598-020-76304-x>

910 Stammer, D., Cazenave, A., Ponte, R.M. and Tamisiea, M.E., 2013. Causes for contemporary regional sea
 911 level changes. *Annual Review of Marine Science*, 5, pp.21-46.

912 Thanh, V. Q., Reyns, J., Van, S. P., Anh, D. T., Dang, T. D., & Roelvink, D. 2019. Sediment transport and
 913 morphodynamical modeling on the estuaries and coastal zone of the Vietnamese Mekong Delta. *Continental*
 914 *Shelf Research*, 186, 64-76.

915 WARPO and BUET, 2019. Research on the Morphological processes under Climate Changes, Sea Level
 916 Rise and Anthropogenic Intervention in the coastal zone, Final Report, March 2019.
 917 [http://warpo.portal.gov.bd/sites/default/files/files/warpo.portal.gov.bd/page/9b4814df_f835_4b0d_8c60_f](http://warpo.portal.gov.bd/sites/default/files/files/warpo.portal.gov.bd/page/9b4814df_f835_4b0d_8c60_f2b35e0343b9/Research_Report.pdf)
 918 [2b35e0343b9/Research_Report.pdf](http://warpo.portal.gov.bd/sites/default/files/files/warpo.portal.gov.bd/page/9b4814df_f835_4b0d_8c60_f2b35e0343b9/Research_Report.pdf)

919 WARPO and BUET, 2020. Research on Sediment Distribution and Management in South-West Region of
 920 Bangladesh, IWMF, BUET, Interim Report, September 2020.

921 WARPO and BUET, 2021. Research on Sediment Distribution and Management in South-West Region of
 922 Bangladesh, Draft Final Report, November 2021.

923 Wilson C., Goodbred S., Small C., Gilligan J., Sams S., Mallick B. and Hale R. 2017. Widespread infilling
 924 of tidal channels and navigable waterways in the human-modified tidal delta plain of southwest Bangladesh.
 925 *Elem Sci Anth*, 5: 78. DOI: <https://doi.org/10.1525/elementa.263>

926 Woodroffe C.D., Nicholls R.J., Saito Y., Chen Z., Goodbred S.L. 2006. Landscape Variability and the
 927 Response of Asian Megadeltas to Environmental Change. In: Harvey N. (eds) *Global Change and*
 928 *Integrated Coastal Management. Coastal Systems and Continental Margins*, vol 10. Springer, Dordrecht.
 929 https://doi.org/10.1007/1-4020-3628-0_10

930 World Bank, 2012. Annual Report, Bangladesh Climate Change Resilience Fund,
931 <https://documents1.worldbank.org/curated/en/697541468198577760/pdf/692500AR00PUBL01100Feb01>
932 20020120020.pdf
933 Zhang, H., Nakagawa, H., Baba, Y., Kawaike, K. and Teraguchi, H., 2010. Three Dimensional Flow
934 around Bandal-like Structures, Annual Journal of Hydraulic Engineering, JSCE, Vol.54, pp.175-180, 2010,
935 February.
936